Continuous-time quantum walks in phase space

Oliver Mülken and Alexander Blumen

Theoretische Polymerphysik, Universität Freiburg, Hermann-Herder-Straße 3, D-79104 Freiburg, Germany
(Received 21 September 2005; published 11 January 2006)

We formulate continuous time quantum walks (CTQW) in a discrete quantum mechanical phase space. We define and calculate the Wigner function (WF) and its marginal distributions for CTQWs on circles of arbitrary length N. The WF of the CTQW shows characteristic features in phase space. Revivals of the probability distributions found for continuous and for discrete quantum carpets do manifest themselves as characteristic patterns in phase space.

I. INTRODUCTION

The study of quantum mechanical transport phenomena on discrete structures is of eminent interest. One particular aspect is the crossover from quantum mechanical to classical behavior. Since classical physics is described in phase space and quantum mechanics in Hilbert space, a unified picture is desired. This is provided, for instance, by the so-called Wigner function (WF) [1,2], which has remarkable properties: It transforms the wave function of a quantum mechanical particle into a function living in a position-momentum space similar to the classical phase space. The WF is a real valued function and in this respect compares well with the classical probability density in phase space. However, it is not always positive.

The concept of phase space functions has been widely used in quantum optics [3,4] and also for describing electronic transport, see, e.g., Refs. [5–7]. Here, the formal similarity to the classical Boltzmann distribution has been exploited. However, the phase spaces considered there are mostly continuous and infinite. This results in a simpler mathematical tractability of WFs than for discrete and for finite systems. Nevertheless, one can also define WFs for discrete systems [8–12].

Describing the transport by coined or continuous-time quantum walks has been very successful over the past few years; for an overview, see Ref. [13]. The applicability of quantum walks reaches far beyond quantum computation; for instance, in quantum optics also the (discrete) Talbot effect can be described by continuous-time quantum walks [14,15]. An additional but more abstract approach to transport processes is through the so-called quantum multibaker maps [16,17]. Such maps were shown to exhibit (as a function of time) a quantum-classical crossover, where the crossover time is given by the inverse of Planck's constant.

In the following we define the WF for a continuous-time quantum walk on a one-dimensional discrete network of arbitrary length N with periodic boundary conditions (PBC). We further show that the marginal distributions are correctly reproduced. Additionally, we define a long time average of the WF, which we compare to the classical limiting phase space distribution. Finally, we show how (partial) revivals of the probability distribution manifest themselves in phase space.

II. CONTINUOUS-TIME QUANTUM WALKS

The quantum mechanical extension of a continuous-time random walk (CTRW) on a network (graph) of connected nodes is called a continuous-time quantum walk (CTQW). It is obtained by identifying the Hamiltonian of the system with the (classical) transfer matrix, $\mathbf{H} = -\mathbf{T}$; see, e.g., Refs. [18] and [19] (we will set $\hbar \equiv 1$ in the following). The transfer matrix of the walk, $\mathbf{T} = (T_{ij})$, is related to the adjacency matrix $\mathbf{A}$ of the graph by $\mathbf{T} = -\gamma\mathbf{A}$, where for simplicity we assume the transmission rate γ of all bonds to be equal. The matrix $\mathbf{A}$ has as nondiagonal elements A_{ij} the values -1 if nodes i and j of the graph are connected by a bond and 0 otherwise. The diagonal elements A_{ii} of $\mathbf{A}$ equal the number of bonds f_i which exit from node i.

The basis vectors $|j\rangle$ associated with the nodes j span the whole accessible Hilbert space to be considered here. The time evolution of a state $|j\rangle$ starting at time t_0 is given by $|j;t\rangle = \mathbf{U}(t,t_0)|j\rangle$, where $\mathbf{U}(t,t_0) = \exp[-i\mathbf{H}(t-t_0)]$ is the quantum mechanical time-evolution operator.

III. WIGNER FUNCTIONS

A. Definition

The WF is a quasiprobability (in the sense that it can become negative) in the quantum mechanical phase space. For a d dimensional system, the (quantum mechanical) phase space is $2d$ dimensional. If the phase space is spanned by the continuous variables X and K, the WF is given by [1,2]

$$W(X,K;t) = \frac{1}{\pi} \int dY\, e^{iKY}\langle X - Y/2|\hat{\rho}(t)|X + Y/2\rangle, \quad (1)$$

where $\hat{\rho}(t)$ is the density operator and thus for a pure state, $\hat{\rho}(t) = |\psi(t)\rangle\langle\psi(t)|$. Here, $\psi(X;t) = \langle X|\psi(t)\rangle$ is the wave function of the particle. Integrating $W(X,K;t)$ along lines in phase space gives marginal distributions, e.g., when integrating along the K axis one has [1,2],

$$\int dK\, W(X,K;t) = |\psi(X;t)|^2. \quad (2)$$

In the case of a discrete system, given, for instance, by N discrete positions on a network, which we choose to enumerate as $0, 1, \ldots, N-1$, the functions $\psi(x)$ are only defined for

integer values of $x=0,1,\ldots,N-1$, and the form of Eq. (1) has to be changed from an integral to a sum. There have been several attempts in doing so; see, for instance, Refs. [8] and [9]. However, the definition of the discrete WFs might depend on whether the length N of the system is even or odd [10,20].

In the following we proceed somewhat differently than previous works and focus on discrete systems with PBC. For a one-dimensional system of length N (exemplified by a ring) this implies $\psi(x)\equiv\psi(x\pm rN)$ for all $r\in\mathbb{N}$. It follows that each and every one of the products $\psi^*(x-y';t)\psi(x+y';t)$ is identical to (at least) one of the N forms $\psi^*(x-y;t)\psi(x+y;t)$, where $y=0,1,\ldots,N-1$.

Now the WF has the form of a Fourier transform; a unique transformation of these N products requires N different k values. These k values may evidently be chosen as $k=2\pi\kappa/N$, again having $\kappa=0,1,\ldots,N-1$. We are thus led to propose for integer x and y the following discrete WF:

$$W(x,k;t)=\frac{1}{N}\sum_{y=0}^{N-1} e^{iky}\psi^*(x-y;t)\psi(x+y;t). \quad (3)$$

As a side remark we note that the right-hand side (rhs) of Eq. (3) stays invariant when replacing N by mN (with m integer and $m\neq 0$). Furthermore, also the choice of the summation interval $0,1,\ldots,N-1$ is arbitrary; any N consecutive y values will do. Given that the nature of the Hilbert space underlying Eq. (1) differs from that of Eq. (3), there is no simple relation connecting the two equations. Here, one may recall the problem of the normalization of plane waves in bounded (compact) and in infinite spaces. In the following we will use Eq. (3) in order to compute the WFs.

B. WFs and the Bloch ansatz

In the following we consider only CTQWs with nearest neighbor steps. The Hamilton operator for such a CTQW on a finite one-dimensional network with PBC takes on a very simple form,

$$\mathbf{H}|j\rangle=2|j\rangle-|j-1\rangle-|j+1\rangle, \quad (4)$$

where we have taken the transmission rate to be $\gamma\equiv 1$. The states $|j\rangle$, where $j=0,1,\ldots,N-1$, are the basis states associated with the nodes j. Since here the CTQW describes a particle moving in a periodic potential we can employ the Bloch ansatz [15,21]. The time independent Schrödinger equation $\mathbf{H}|\Phi_\theta\rangle=E_\theta|\Phi_\theta\rangle$ has eigenstates $|\Phi_\theta\rangle$ which are Bloch states. The PBC require that $\Phi_\theta(N)=\Phi_\theta(0)$, where $\Phi_\theta(x)=\langle x|\Phi_\theta\rangle$. As before, this restricts the θ values to $\theta=2\pi n/N$, where $n=0,1,\ldots,N-1$. The Bloch state $|\Phi_\theta\rangle$ can be expressed as a linear combination of the states $|j\rangle$,

$$|\Phi_\theta\rangle=\frac{1}{\sqrt{N}}\sum_{j=0}^{N-1} e^{i\theta j}|j\rangle. \quad (5)$$

In turn, the state $|j\rangle$ can be expressed by the Bloch states, i.e., by a Wannier function [21],

$$|j\rangle=\frac{1}{\sqrt{N}}\sum_\theta e^{-i\theta j}|\Phi_\theta\rangle, \quad (6)$$

where the sum runs over the N values for θ. From this it follows readily that the eigenvalues to Eq. (4) are given by $E_\theta=2-2\cos\theta$. The time evolved state then follows as

$$|j;t\rangle\equiv e^{-i\mathbf{H}t}|j\rangle=\frac{1}{\sqrt{N}}\sum_\theta e^{-i\theta j}e^{-iE_\theta t}|\Phi_\theta\rangle, \quad (7)$$

Using the position basis means introducing $\psi_j(x;t)\equiv\langle x|j;t\rangle$. Evidently, at $t=0$ one has $\psi_j(x;0)=\langle x|j\rangle=\delta_{x,j}$. Furthermore, with Eq. (7) we have

$$
\begin{aligned}
\psi_j^*(x';t)\psi_j(x;t)&\equiv\langle j;t|x'\rangle\langle x|j;t\rangle\\
&=\frac{1}{N}\sum_{\theta,\theta'} e^{-i(\theta-\theta')j}e^{i(E_{\theta'}-E_\theta)t}\Phi_{\theta'}^*(x')\Phi_\theta(x)\\
&=\frac{1}{N^2}\sum_{\theta,\theta'} e^{-i(\theta-\theta')j}e^{i(E_{\theta'}-E_\theta)t}\\
&\quad\times\sum_{l,l'} e^{il\theta}e^{-il'\theta'}\delta_{x',l'}\delta_{x,l}\\
&=\frac{1}{N^2}\sum_{\theta,\theta'} e^{-i(\theta-\theta')j}e^{i(E_{\theta'}-E_\theta)t}e^{i\theta x}e^{-i\theta'x'}. \quad (8)
\end{aligned}
$$

Now, following Eq. (3), the WF is given by

$$W_j(x,k;t)=\frac{1}{N^3}\sum_{\theta,\theta'} e^{i(\theta-\theta')(x-j)}e^{i(E_{\theta'}-E_\theta)t}\sum_y e^{i(\theta+\theta'+k)y}. \quad (9)$$

The sum over y can be written as $N\Delta_{\theta+\theta'+k}$, where, as an extension of the usual Kronecker symbol, we introduce $\Delta_n=1$ for $n\equiv 0\pmod N$ and $\Delta_n=0$ else. Therefore, the WF for a CTQW on a one-dimensional network of N nodes with PBC reads

$$
\begin{aligned}
W_j(x,\kappa;t)=\frac{1}{N^2}\sum_{n=0}^{N-1} &\exp[-i2\pi(2n+\kappa)(x-j)/N]\\
&\times\exp(-i2t\{\cos[2\pi(\kappa+n)/N]\\
&-\cos(2\pi n/N)\}), \quad (10)
\end{aligned}
$$

where we have used that $\theta=2\pi n/N$ and $k=2\pi\kappa/N$. Furthermore, one may note from Eq. (3) that

$$
\begin{aligned}
\sum_\kappa W_j(x,\kappa;t)&=\frac{1}{N}\sum_\kappa\sum_y e^{i2\pi\kappa y/N}\psi^*(x-y;t)\psi(x+y;t)\\
&=|\psi(x;t)|^2. \quad (11)
\end{aligned}
$$

Note that the WF in Eq. (10) does not change with time for $\kappa=0$, i.e., we have $W_j(x,0;t)=W_j(x,0;0)=\mathcal{W}_j(x,0)$, where $\mathcal{W}_j(x,\kappa)$ is the long time average of the WF given in Sec. IV C.

IV. WFs AND CTQWs

In the following we consider WFs for CTQWs on circles of different length. For $t=0$ we start the CTQWs from one
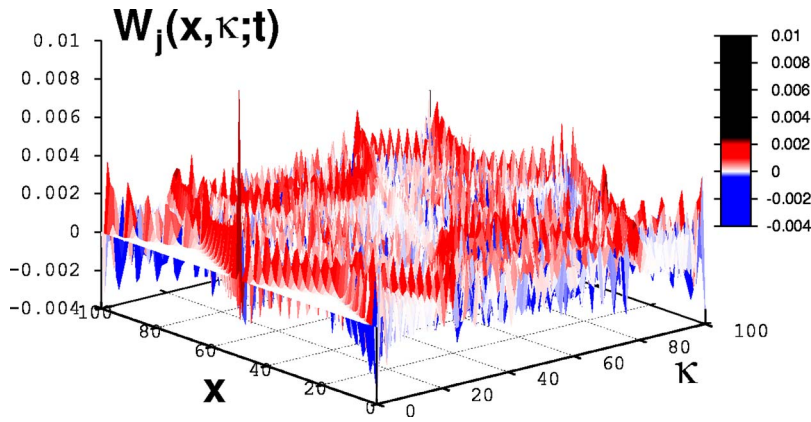
FIG. 1. (Color online) 3D visualization of the WFs of a CTQW on a cycle of length $N=101$ at $t=40$. The initial node is at $j=50$.

node. In particular, we take $N=100$ (as an example of an even value) and $N=101$ (as odd value); as starting site, we choose $j=50$.

A. CTQWs in phase space

In general, the WFs have a very complex structure. Figures 1 and 2 display the WFs for CTQWs over cycles with $N=101$ and $N=100$, respectively, at $t=40$. The peaks at $(x,\kappa)=(j,0)$ for $N=101$ and for $N=100$ are clearly noticeable (black peaks in Figs. 1 and 2); however, the remaining structure is quite complex.

Figure 3 shows a contour plot of the WF of a CTQW on a cycle of length $N=101$ at different times. Note that at $t=0$ the WF is localized on the strip at the initial point j. At $t=1$, the WF is still mostly localized about j. As time increases, other sites get populated. On short time scales, the WF develops a very regular structure in phase space, with "wave fronts" originating from the initial point j. Additionally, we also note wave fronts starting from the region opposite to the initial point, which are much weaker in amplitude. As time progresses, these two types of waves start "interfering" with each other.

In Fig. 4 we plot the WF of a CTQW for $N=100$. The structure of the WF is quite similar to the odd-numbered network. Nonetheless, there are differences at larger times, visible by comparing Figs. 3(e) and 3(f) to Figs. 4(e) and 4(f).

However, although at long times the interference effects are quite intricate, typical patterns are still visible.

At $t=500$, we find less regularities in phase space for $N=101$ than for $N=100$, reflecting the higher symmetry of CTQWs on even-numbered networks. We note, moreover, that the phase space pictures give at any time a much richer picture of the underlying dynamics than the transition probabilities $|\psi_j(x;t)|^2$ alone. While the transition probabilities appear to be quite irregular [15], the WFs display regular patterns. As in the case of a particle in the box [22], also here we might view the ensuing structure, the "quantum carpets," to be woven by the discrete WFs.

We finally note that in an infinite system the WFs have a much simpler structure, because there we do not face the problem of distinct wave fronts running into opposite directions and interfering with each other.

B. Marginal distributions

In general, the marginal distribution $\Sigma_\kappa W_j(x,\kappa;t)$ is obtained from Eq. (10) as

$$
\begin{aligned}
\sum_\kappa W_j(x,\kappa;t) &= \frac{1}{N}\sum_{n=0}^{N-1} \exp[-i2\pi n(x-j)/N] \\
&\times \exp[i2t\cos(2\pi n/N)] \\
&\times \frac{1}{N}\sum_{\kappa=0}^{N-1} \exp[-i2\pi(\kappa+n)(x-j)/N] \\
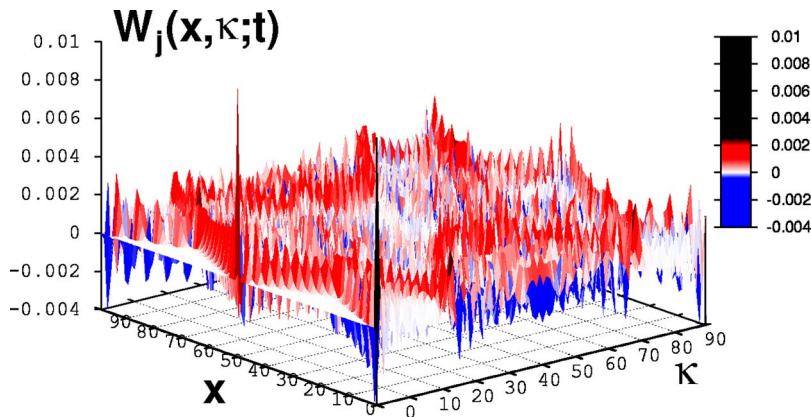&\times \exp[-i2t\cos(2\pi(\kappa+n)/N)]. \quad (12)
\end{aligned}
$$

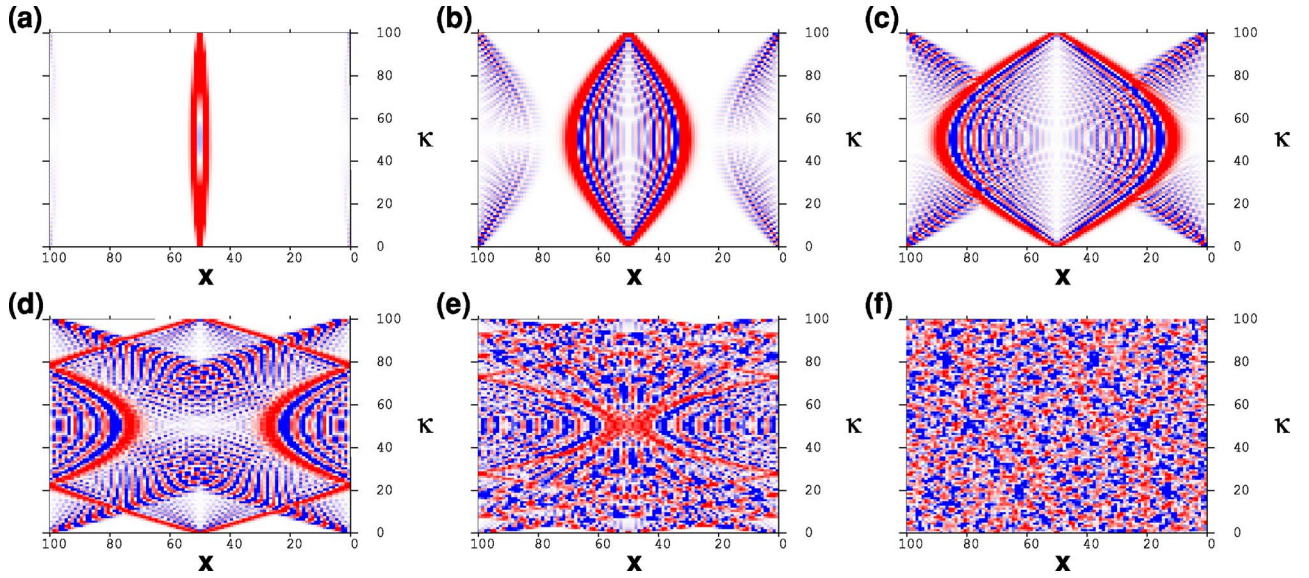FIG. 2. (Color online) Same as Fig. 1, for $N=100$ at $t=40$ with $j=50$.

FIG. 3. (Color online) WFs of a CTQW on a cycle of length $N=101$ at times $t=1,10,20,40$ [(a)–(d)] as well as $t=100,500$ [(e),(f)]. The initial node is at $j=50$. Red regions denote positive values of $W_j(x,\kappa;t)$, blue regions negative values, and white regions values close to 0.

Since the system is periodic, the arguments $(\kappa+n)$ in the exponentials can be substituted by $(\kappa+n)\equiv N-\nu$, where $\nu=0,1,\ldots,N-1$. This yields

$$\sum_\kappa W_j(x,\kappa;t) = \left| \frac{1}{N}\sum_{\nu=0}^{N-1} e^{i2\pi\nu(x-j)/N}e^{-i2t\cos(2\pi\nu/N)} \right|^2, \quad (13)$$

which is exactly what also follows, see Eq. (11), from calculating $|\psi(x;t)|^2$ directly from the Bloch ansatz, see Eq. (8). The same relation was also highlighted in Ref. [15].

Furthermore, we obtain the marginal distribution $\Sigma_\kappa W_j(x,\kappa;t)$ for the infinite system by taking N large (but fixed) in Eq. (13), and setting $\theta=2\pi\nu/N$. We are then led to

$$\sum_\kappa W_j(x,\kappa;t) = \left| \frac{1}{2\pi}\int_0^{2\pi} d\theta\, e^{i\theta(x-j)}e^{-i2t\cos\theta} \right|^2 = [J_{x-j}(2t)]^2,$$

(14)

where $J_\nu(\tau)$ is the Bessel function of the first kind [see Eq. (9.1.21) of Ref. [23]].

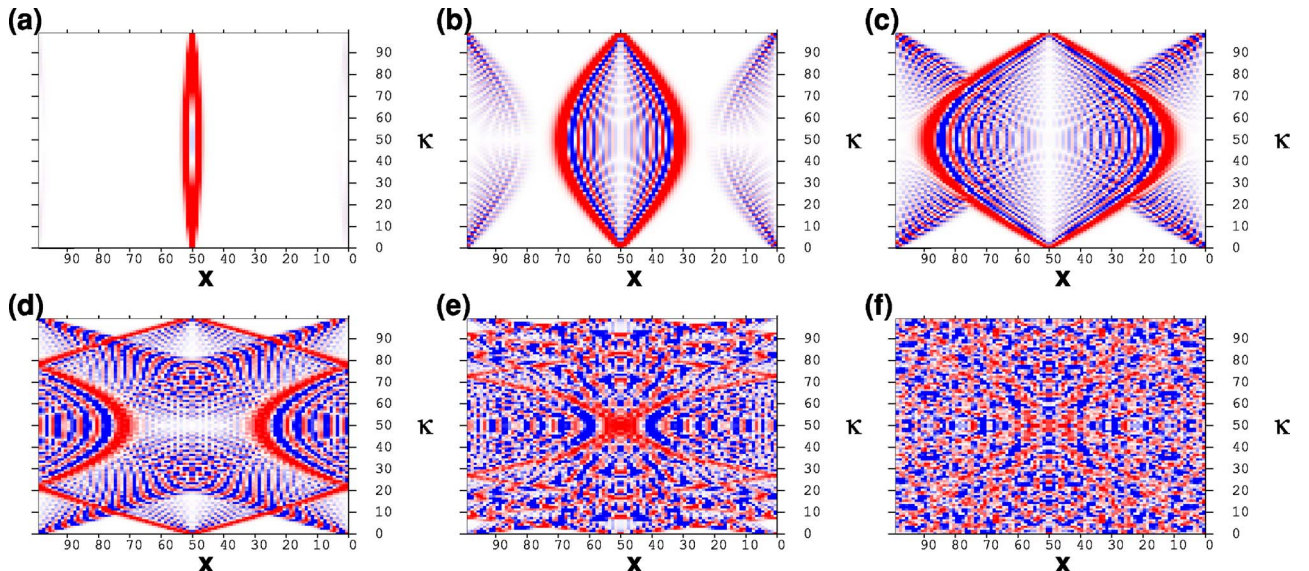For the marginal distribution $\Sigma_x W_j(x,\kappa;t)$ we also get from Eq. (10)

FIG. 4. (Color online) Same as Fig. 3, for $N=100$ and $j=50$.

$$\sum_x W_j(x,\kappa;t) = \frac{1}{N^2}\sum_{n=0}^{N-1} N\Delta_{2n+\kappa}e^{i2\pi(2n+\kappa)j/N}\exp(-i2t$$

$$\times\{\cos[2\pi(\kappa+n)/N] - \cos(2\pi n/N)\})$$

$$= \begin{cases} 1/N & N \text{ odd and all } \kappa \\ 2/N & N \text{ even and } \kappa \text{ even} \\ 0 & N \text{ even and } \kappa \text{ odd}, \end{cases} \qquad (15)$$

which is independent of t. Equation (15) can be confirmed directly by taking the Fourier transform of $|\psi(x;t)|^2$. The whole phase space volume is normalized to one, as can be seen by summing Eq. (15) over all κ, with $\kappa=0,1,\ldots,$ $N-1$.

C. Long time averages

Similar to the classical case, the CTQW will visit any point in phase space. However, due to the evolution with the unitary **H**, there is no definite limiting distribution. For the CTQW one may view the long time average of the transition probability $|\psi_j(x;t)|^2$ as a limiting distribution [24], i.e.,

$$\chi_{xj} \equiv \lim_{T\to\infty} \frac{1}{T}\int_0^T dt\,|\psi_j(x;t)|^2. \qquad (16)$$

Employing this idea, we define the limiting WF as

$$\mathcal{W}_j(x,\kappa) \equiv \lim_{T\to\infty} \frac{1}{T}\int_0^T dt\,W_j(x,\kappa;t). \qquad (17)$$

Upon integration of Eq. (10) over t the only term which remains is the one for which $\cos[2\pi(\kappa+n)/N]$ $=\cos[2\pi n/N]$.

Some care is in order here, since for the long time average there are differences between even and odd N, also occurring in the limiting distribution χ_{xj} [15]. In the case of an odd N (superscript ^{o}) we get

$$\mathcal{W}_j^o(x,\kappa) = \begin{cases} 1/N^2 & \kappa \neq 0 \text{ and any } x \\ 1/N & \kappa = 0 \text{ and } x = j \\ 0 & \text{else.} \end{cases} \qquad (18)$$

Note that for $k \neq 0$ we require $2n=N-\kappa$.

For an even N (superscript ^{e}), the limiting WF for $\kappa=0$ has contributions only for $x=j$ and $x=j+N/2$. Each of the two contributions has weight $1/2$. Thus the limiting WF reads

$$\mathcal{W}_j^e(x,\kappa) = \begin{cases} 1/N^2 & \kappa \neq 0 \text{ and any } x \\ 1/2N & \kappa = 0 \text{ and } x = j, j+N/2 \\ 0 & \text{else.} \end{cases} \qquad (19)$$

Note that also here we require that $2n=(N-k)$

The long time average of the WF is always positive. Note that for classical CTRWs the limiting phase space distribution is uniform and equals $1/N^2$ both for odd *and* for even N. Thus, what distinguishes the limiting WF from the classical limiting distribution are a few exceptional points in the phase space.
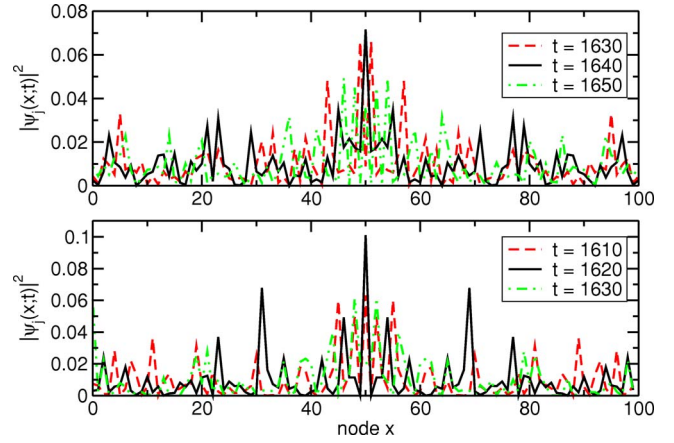

FIG. 5. (Color online) Transition probability $|\psi_j(x;t)|^2$ as function of x of CTQWs on cycles of length (a) $N=101$ at times $t=1620,1640,1650$ and (b) $N=100$ at times $t=1610,1620,1630$. The initial node is $j=50$ in both cases.

The long time average of the marginal distribution $|\psi_j(x;t)|^2$ is also recovered from the limiting WF as $\sum_\kappa \mathcal{W}_j(x,\kappa)=\chi_{xj}$, thus for odd N

$$\chi_{xj}^o = \begin{cases} (2N-1)/N^2 & \text{for } x=j \\ (N-1)/N^2 & \text{else,} \end{cases} \qquad (20)$$

and for even N

$$\chi_{xj}^e = \begin{cases} (2N-2)/N^2 & \text{for } x=j, j+N/2 \\ (N-2)/N^2 & \text{else} \end{cases}, \qquad (21)$$

which confirms our previous calculations [15]

D. Revivals in phase space

CTQWs on large networks show only partial revivals [15]. These should occur at times $t_r \gtrsim N^2/2\pi$. However, for small networks of sizes $N=1,2,3,4,6$ complete revivals are also possible, as was recently seen in waveguide arrays [14]. The WFs are easily obtained from Eq. (10). The marginal distributions $\sum_\kappa W_j(x,\kappa;t)$ are, of course, correctly recovered. For instance, for $N=6$, the first complete revival occurs for $t=2\pi$. This is readily seen, since for the WF at $x=j$ we have $W_j(x=j,\kappa;t=2\pi)=1/6$; thus the marginal distribution is $\sum_\kappa W_j(x=j,\kappa;t=2\pi)=1$, which also means, using Eq. (11), that $|\psi_j(x=j;t=2\pi)|^2=1$.

Figure 5 shows the transition probability $|\psi_j(x;t)|^2$ for $N=101$ and $N=100$ at three different times t close to the corresponding t_r. For $N=101$ ($N=100$) at $t=1640$ ($t=1620$) the CTQW shows the closest revival to the initial distribution $|\psi_j(x;0)|^2$ in that time interval. The corresponding phase space pictures are given in Fig. 6.

Although the phase space pictures in Fig. 6 are vastly different from the ones at the initial time, there are strong peaks in the WFs seen as red regions close to the initial point, $j=50$. Moreover, the patterns in Figs. 6(a) and 6(b) are more regular than, say, the ones in Figs. 3(f) and 4(f). Especially along lines perpendicular to the initial node j, there are in both cases areas with strong positive peaks in the WF,
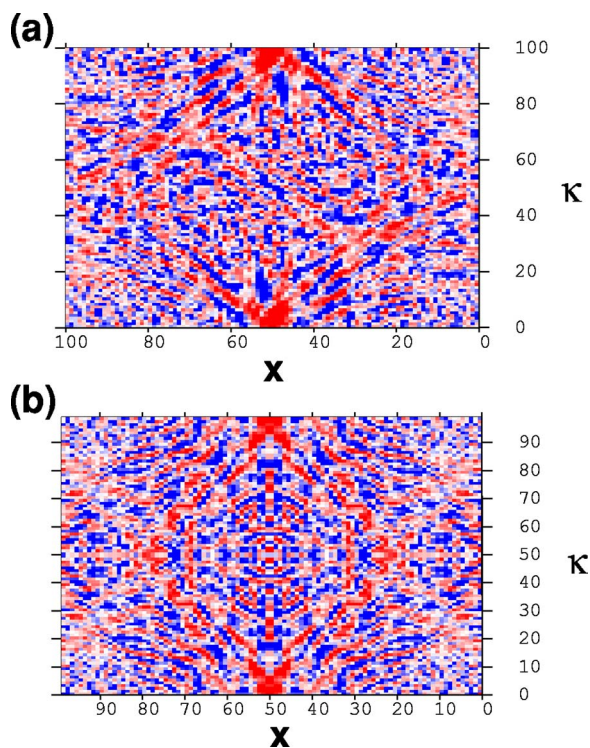
FIG. 6. (Color online) WFs of a CTQW on a cycle of length (a) $N=101$ at time $t=1640$ and (b) $N=100$ at time $t=1620$. The initial node is $j=50$ in both cases. Red regions denote positive values, blue regions negative values, and white regions values close to 0 of $W_j(x,\kappa;t)$.

giving rise to strong peaks in the marginal distribution $\Sigma_\kappa W_j(x,\kappa;t)$. All this means that close to a partial revival the structure is by far more regular than at an arbitrary moment in time.

V. CONCLUSIONS

In conclusion, we have defined and calculated the discrete WF of a CTQW on a discrete cycle of arbitrary length N with PBC. Different from previous attempts, our definition is independent of whether N is even or odd. Integrating the WF along lines in phase space gives the correct marginal distributions. The WF exhibits characteristic patterns. Furthermore, we also showed how partial revivals of the WF manifest themselves in phase space. The patterns in phase space allow us to draw a much richer picture of the CTQW than the marginal distributions can.

ACKNOWLEDGMENTS

[1] E. P. Wigner, Phys. Rev. **40**, 749 (1932).
[2] M. Hillery, R. F. O'Connell, M. O. Scully, and E. P. Wigner, Phys. Rep. **106**, 121 (1984).
[3] W. P. Schleich, *Quantum Optics in Phase Space* (Wiley-VCH, Berlin, 2001).
[4] L. Mandel and E. Wolf, *Optical Coherence and Quantum Optics* (Cambridge University Press, Cambridge, England, 1995).
[5] N. C. Kluksdahl, A. M. Kriman, D. K. Ferry, and C. Ringhofer, Phys. Rev. B **39**, 7720 (1989).
[6] F. A. Buot, Phys. Rep. **234**, 73 (1993).
[7] P. Bordone, M. Pascoli, R. Brunetti, A. Bertoni, C. Jacoboni, and A. Abramo, Phys. Rev. B **59**, 3060 (1999).
[8] W. K. Wootters, Ann. Phys. **176**, 1 (1987).
[9] O. Cohendet, P. Combe, M. Sirugue, and M. Sirugue-Collin, J. Phys. A **21**, 2875 (1988).
[10] U. Leonhardt, Phys. Rev. Lett. **74**, 4101 (1995).
[11] A. Takami, T. Hashimoto, M. Horibe, and A. Hayashi, Phys. Rev. A **64**, 032114 (2001).
[12] C. Miquel, J. P. Paz, and M. Saraceno, Phys. Rev. A **65**, 062309 (2002).
[13] J. Kempe, Contemp. Phys. **44**, 307 (2003).
[14] R. Iwanow, D. A. May-Arrioja, D. N. Christodoulides, G. I. Stegeman, Y. Min, and W. Sohler, Phys. Rev. Lett. **95**, 053902 (2005).
[15] O. Mülken and A. Blumen, Phys. Rev. E **71**, 036128 (2005).
[16] D. K. Wójcik and J. R. Dorfman, Phys. Rev. E **66**, 036110 (2002).
[17] D. K. Wójcik and J. R. Dorfman, Phys. Rev. Lett. **90**, 230602 (2003).
[18] E. Farhi and S. Gutmann, Phys. Rev. A **58**, 915 (1998).
[19] O. Mülken and A. Blumen, Phys. Rev. E **71**, 016101 (2005).
[20] U. Leonhardt, Phys. Rev. A **53**, 2998 (1996).
[21] J. M. Ziman, *Principles of the Theory of Solids* (Cambridge University Press, Cambridge, England, 1972).
[22] O. M. Friesch, I. Marzoli, and W. P. Schleich, New J. Phys. **2**, 4.1 (2000).
[23] *Handbook of Mathematical Functions*, edited by M. Abramowitz and I. A. Stegun (Dover, New York, 1972).
[24] D. Aharonov, A. Ambainis, J. Kempe, and U. Vazirani, in *Proceedings of ACM Symposium on Theory of Computation (STOC '01)* (ACM Press, New York, 2001), p. 50.